Structure and Reactivity of Chelating Imido−Amido Complexes of Tantalum. Mechanistic Studies on the Addition of Silanes to Ta−N Multiple Bonds

Tomislav I. Gountchev and T. Don Tilley*

Contribution from the Department of Chemistry, University of California, Berkeley, Berkeley, California 94720-1460

Received July 2, 1997[⊗]

Abstract: The synthesis, structural characterization, and reactivity of tantalum complexes with chelating imido−amido ligands are reported. The highly bent imido complex Cp*Ta[=N(C_6H_3Me)$_2$NSiMe$_3$]Cl (**4**, Cp* = η^5-C_5Me_5), with a Ta=N−C bond angle of 116.3(4)°, was synthesized from Cp*$TaCl_4$ and the lithiated bis(silylamino)-biphenyl (C_6H_3Me)$_2$(NLiSiMe$_3$)$_2$ (**3**). Compound **4** undergoes reactions with electrophiles at the nucleophilic imido nitrogen atom. The methyl derivative Cp*Ta[=N(C_6H_3Me)$_2$NSiMe$_3$]Me (**5**) reacts with xylyl isonitrile to give an insertion product, **6**, which was structurally characterized. Addition of MeI to **5** gives a cationic diamide tantalum complex, {Cp*Ta[MeN(C_6H_3Me)$_2$NSiMe$_3$]Me}$^+$I$^-$ (**7**), the ionic structure of which was confirmed by X-ray crystallography. Reactions of **4** and **5** with unhindered silanes result in addition of the silane Si−H bond across the Ta=N double bond. Addition of $PhSiH_3$ to **4** and **5** gave the hydrides Cp*Ta[$PhSiH_2$N(C_6H_3Me)$_2$NSiMe$_3$](H)Cl (**8**) and Cp*Ta[$PhSiH_2$N(C_6H_3Me)$_2$NSiMe$_3$](H)Me (**9**), respectively. The crystal structure of **9** was determined. Compounds **8** and **9** are unstable and decompose via elimination of $HSiMe_3$. In the presence of CH_2Cl_2 and $PhSiH_3$, **4** was slowly converted to another hydrido complex, Cp*Ta[$PhSiH_2$N(C_6H_3Me)$_2$NSiPhHCl](H)Cl (**12**). A mechanism for this transformation, involving a sequence of silane addition/elimination reactions, is proposed. X-ray structural characterization of **12** revealed the presence of a nonclassical bonding interaction between the hydride ligand and a neighboring silyl group, leading to a short H−Si contact of 1.86(4) Å and a distorted pentagonal bipyramidal geometry at silicon. Reactions of $PhSiH_3$ and $(CH_2)_3SiH_2$ (silacyclobutane) with **5** follow second-order kinetics, and an inverse deuterium isotope effect of k_H/k_D = 0.78(1) for the addition of $PhSiH_3$ to **5** was observed. The elimination of $HSiMe_3$ from **9** was found to follow a first-order rate law with approach to equilibrium (K_H = 0.025(2) mol/L) and exhibit an inverse isotope effect of k_H/k_D = 0.85(2). A study of the temperature dependence of the first-order rate constant for $HSiMe_3$ elimination from **9** provided the activation parameters $\Delta H^{\ddagger}$= 25.5(3) kcal/mol and $\Delta S^{\ddagger}$ = −0.3(1.0) cal/(mol·K). These findings are interpreted in terms of a mechanism involving slow, rate-determining formation of pentacoordinate silicon intermediates, coupled with a fast hydride shift between Ta and Si.

Introduction

Early-transition-metal chemistry has received increased attention in recent years, particularly as new applications in catalysis and polymer chemistry have been developed.[1−9] Much of this new chemistry involves metal complexes which possess cyclopentadienyl ligand sets. Such complexes are readily modified to adjust electronic and steric properties for the metal center and, therefore, activities and selectivities for the catalyst.[2,3] Many of the systems of interest involve electrophilic and coordinatively unsaturated d^0 metal centers that behave as Lewis acids in their chemistry. For this reason, effort has been devoted to development of alternative ligand sets that may increase the electrophilicity of the metal center.[10−14] One approach involves use of ancillary multidentate amido ligands to support reactive and highly electrophilic metal centers.[13−26]

In our investigations on alternative ancillary ligands for d^0

⊗ Abstract published in *Advance ACS Abstracts,* December 15, 1997.

(1) Brintzinger, H. H.; Fischer, D.; Mulhaupt, R.; Rieger, B.; Waymouth, R. *Angew. Chem., Int. Ed. Engl.* **1995**, *34*, 1143.
(2) Kaminsky, W. *Catal. Today* **1994**, *20*, 257.
(3) Möhring, P. C.; Coville, N. J. *J. Organomet. Chem.* **1994**, *479*, 1.
(4) Tilley, T. D. *Acc. Chem. Res.* **1993**, *26*, 22.
(5) Dioumaev, V. K.; Harrod, J. F. *J. Organomet. Chem.* **1996**, *521*, 133.
(6) Jordan, R. F. *Adv. Organomet. Chem.* **1991**, *32*, 325.
(7) Marks, T. J. *Acc. Chem. Res.* **1992**, *25*, 57.
(8) Visciglio, V. M.; Clark, J. R.; Nguyen, M. T.; Mulford, D. R.; Fanwick, P. E.; Rothwell, I. P. *J. Am. Chem. Soc.* **1997**, *119*, 3490.
(9) Verdaguer, X.; Lange, U. E. W.; Reding, M. T.; Buchwald, S. L. *J. Am. Chem. Soc.* **1996**, *118*, 6784.
(10) van der Linden, A.; Schaverien, C. J.; Meijboom, N.; Ganter, C.; Orpen, A. G. *J. Am. Chem. Soc.* **1995**, *117*, 3008.
(11) Duchateau, R.; van Wee, C. T.; Meetsma, A.; van Duijnen, P. T.; Teuben, J. H. *Organometallics* **1996**, *15*, 2279.
(12) Rodriguez, G.; Bazan, G. C. *J. Am. Chem. Soc.* **1997**, *119*, 343.
(13) Baumann, R.; Davis, W. M.; Schrock, R. R. *J. Am. Chem. Soc.* **1997**, *119*, 3830.
(14) Schrock, R. R. *Acc. Chem. Res.* **1997**, *30*, 9.
(15) Scollard, J. D.; McConville, D. H.; Payne, N. C.; Vittal, J. J. *Macromolecules* **1996**, *29*, 5241.
(16) Guérin, F.; McConville, D. H.; Payne, N. C. *Organometallics* **1996**, *15*, 5085.
(17) Clark, H. C. S.; Cloke, F. G. N.; Hitchcock, P. B.; Love, J. B.; Wainwright, A. P. *J. Organomet. Chem.* **1995**, *501*, 333.
(18) Scollard, J. D.; McConville, D. H.; Vittal, J. J. *Organometallics* **1995**, *14*, 5478.
(19) Horton, A. D.; de With, J.; van der Linden, A. J.; van de Weg, H. *Organometallics* **1996**, *15*, 2672.
(20) Cloke, F. G. N.; Hitchcock, P. B.; Love, J. B. *J. Chem. Soc., Dalton Trans.* **1995**, 25.
(21) VanderLende, D. D.; Abboud, K. A.; Boncella, J. M. *Organometallics* **1994**, *13*, 3378.
(22) Deelman, B.-J.; Hitchcock, P. B.; Lappert, M. F.; Lee, H.-K.; Leung, W.-P. *J. Organomet. Chem.* **1996**, *513*, 281.
(23) Freundlich, J. S.; Schrock, R. R.; Davis, W. M. *J. Am. Chem. Soc.* **1996**, *118*, 3643.

S0002-7863(97)02198-7 CCC: $14.00

metal centers, we have synthesized and studied a number of complexes with the bis(triisopropylsilyl)-*o*-phenylenediamido (o-$C_6H_4(NSi^iPr_3)_2$) ligand.[27,28] In related efforts, we have been exploring use of C_2-symmetric bis(silylamido) ligands, derived from biphenyl and binaphthyl backbones. The use of similar ligands has recently been reported by Cloke[29] and Lappert.[30] One aspect of this work, reported here, concerns a set of tantalum complexes containing both Cp* (η^5-C_5Me_5) and bis(silylamido) ligands. This system is characterized by facile cleavage of N−Si bonds in the ligand and formation of Ta═N double bonds with unusually acute Ta═N−C bond angles. While this reactivity implies that these silylamides cannot always be regarded as innocent spectator ligands, it presents us with the opportunity to explore the chemistry of a reactive d^0 Ta═N bond. The elimination of silyl groups from silylamido complexes has previously been reported as a limitation in the use of these types of ligands,[14,23] and the cleavage of N−Si bonds has been employed as a route to transition metal imido species.[31−33] However, to our knowledge, the mechanism of this process has not been investigated. Understanding the reactivity of metal−heteroatom multiple bonds is a subject of both theoretical and practical importance. Transition metal imido species[31,32,34] are involved or suspected as intermediates in hydrocarbon activation,[35−39] catalytic hydrodenitrogenation,[40] and hydroamination.[41] Here we describe synthetic and mechanistic studies on the reversible additions of silanes to Ta═N bonds.

Results and Discussion

Ligand Synthesis. The starting material for the synthesis of the target silylamine ligand, 2,2′-diamino-6,6′-dimethylbiphenyl (**1**), was prepared according to literature procedures.[42] *N*-Silylation of this diamine was achieved via deprotonation of **1** in THF followed by reaction of the resulting dianion with Me_3SiCl (eq 1). *N*,*N*′-Bis(trimethylsilyl)-2,2′-diamino-6,6′-dimethylbiphenyl (**2**) was obtained in 84% yield as colorless crystals from pentane. The lithium salt (**3**) was then prepared in 63% yield by treating **2** with 2 equiv of ^{n}BuLi in pentane.

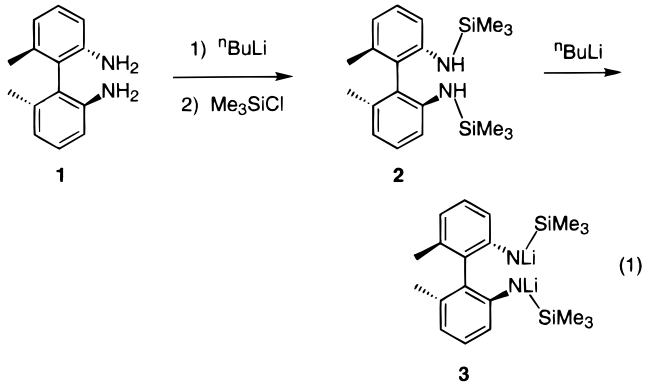

1 2 3 (1)

Syntheses and Characterization of Bent Tantalum Imido Complexes. Reaction of **3** with Cp^*TaCl_4 in refluxing benzene for 4 h yielded a dark red solution. After evaporation of the solvent and extraction with pentane, compound **4** was isolated in 68% yield as a red crystalline powder. ^{1}H NMR spectroscopy indicated that loss of one trimethylsilyl group had occurred to afford a tantalum imido complex, as indicated in eq 2. After 3

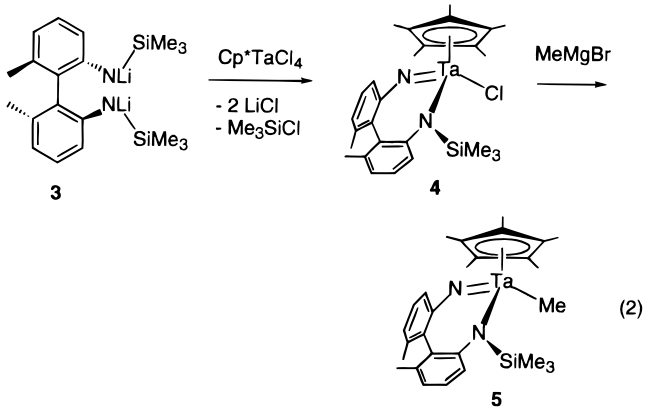

3 4 5 (2)

h (80 °C, benzene-d_6), the reaction had proceeded to >90% conversion with formation of an equimolar mixture of Me_3SiCl and **4**. This reaction therefore differs from that between Cp^*TaCl_4 and o-$C_6H_4(NLiSi^iPr_3)_2$, which produces the stable bis(amido) complex $Cp^*[o\text{-}C_6H_4(NSi^iPr_3)_2]TaCl_2$.[28]

The molecular structure of **4** is shown in Figure 1, and important bond distances and angles are listed in Table 1. The most interesting feature of the molecule is the unusually small Ta−N(1)−C(1) bond angle of 116.3(4)°, which is surprisingly close to the corresponding angle of 114.6(4)° associated with the Ta−N(2)−C(12) amide linkage. The amido N is planar (sum of angles around N(2) = 359.9°), as expected for a metal complex of this type. The Ta═N(1) bond length of 1.830(5) Å is considerably shorter than the Ta−N(2) bond distance of 1.988(6) Å.

The majority of structurally characterized imido complexes exhibit linear, or near linear, geometries with M−N−C bond angles in the range 160−180°.[31,32] The nature of metal−nitrogen bonding in transition metal imido complexes has been the subject of a number of theoretical studies[43−47] which suggest that the metal−ligand bond order is usually intermediate between 2 and 3 and that there is a rather soft potential for

(24) Duan, Z.; Naiini, A. A.; Lee, J.-H.; Verkade, J. G. *Inorg. Chem.* **1995**, *34*, 5477.
(25) Findeis, B.; Schubart, M.; Gade, L. H.; Möller, F.; Scowen, I.; McPartlin, M. *J. Chem. Soc., Dalton Trans.* **1996**, 125.
(26) Schrock, R. R.; Cummins, C. C.; Wilhelm, T.; Lin, S.; Reid, S. M.; Kol, M.; Davis, W. M. *Organometallics* **1996**, *15*, 1470.
(27) Aoyagi, K.; Gantzel, P. K.; Kalai, K.; Tilley, T. D. *Organometallics* **1996**, *15*, 923.
(28) Aoyagi, K.; Gantzel, P. K.; Tilley, T. D. *Polyhedron* **1996**, *15*, 4299.
(29) Cloke, F. G. N.; Geldbach, T. J.; Hitchcock, P. B.; Love, J. B. *J. Organomet. Chem.* **1996**, *506*, 343.
(30) Drost, C.; Hitchcock, P. B.; Lappert, M. F. *J. Chem. Soc., Dalton Trans.* **1996**, 3595.
(31) Nugent, W. A.; Haymore, B. L. *Coord. Chem. Rev.* **1980**, *31*, 123.
(32) Wigley, D. E. *Prog. Inorg. Chem.* **1994**, *42*, 239.
(33) Herrmann, W. A.; Baratta, W. *J. Organomet. Chem.* **1996**, *506*, 357.
(34) Nugent, W. A.; Mayer, J. M. *Metal−Ligand Multiple Bonds*; John Wiley and Sons: New York, 1988.
(35) Schaller, C. P.; Cummins, C. C.; Wolczanski, P. T. *J. Am. Chem. Soc.* **1996**, *118*, 591.
(36) Arndtsen, B. A.; Bergman, R. G.; Mobley, T. A.; Peterson, T. H. *Acc. Chem. Res.* **1995**, *28*, 154.
(37) Walsh, P. J.; Hollander, F. J.; Bergman, R. G. *J. Am. Chem. Soc.* **1988**, *110*, 8729.
(38) de With, J.; Horton, A. D. *Angew. Chem., Int. Ed. Engl.* **1993**, *32*, 903.
(39) Schaller, C. P.; Wolczanski, P. T. *Inorg. Chem.* **1993**, *32*, 131.
(40) Weller, K. J.; Gray, S. D.; Briggs, P. M.; Wigley, D. E. *Organometallics* **1995**, *14*, 5588.
(41) Walsh, P. J.; Baranger, A. M.; Bergman, R. G. *J. Am. Chem. Soc.* **1992**, *114*, 1708.
(42) Kanoh, S.; Goka, S.; Murose, N.; Kubo, H.; Kondo, M.; Sugino, T.; Motoi, M.; Suda, H. *Polym. J.* **1987**, *19*, 1047.
(43) Cundari, T. R. *J. Am. Chem. Soc.* **1992**, *114*, 7879.
(44) Jørgensen, K. A. *Inorg. Chem.* **1993**, *32*, 1521.
(45) Nugent, W. A.; McKinney, R. J.; Kasowski, R. V.; Van-Catledge, F. A. *Inorg. Chim. Acta* **1982**, *65*, L91.
(46) Schofield, M. H.; Kee, T. P.; Anhaus, J. T.; Schrock, R. R.; Johnson, K. H.; Davis, W. M. *Inorg. Chem.* **1991**, *30*, 3595.
(47) Anhaus, J. T.; Kee, T. P.; Schofield, M. H.; Schrock, R. R. *J. Am. Chem. Soc.* **1990**, *112*, 1642.

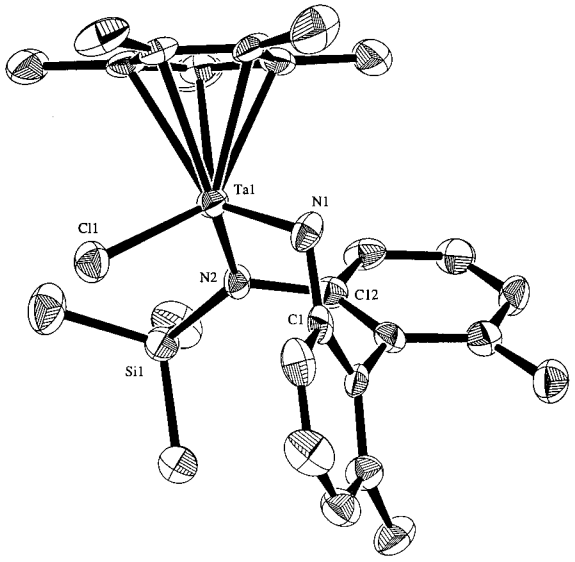

Figure 1. ORTEP diagram of Cp*Ta[=N($C_6H_3Me)_2$NSiMe_3]Cl (**4**).

Table 1. Selected Bond Lengths (Å) and Angles (deg) for Compound **4**

Ta(1)−Cl(1)	2.344(2)	Ta(1)−N(1)-C(1)	116.3(4)
Ta(1)−N(1)	1.830(5)	Ta(1)−N(2)−C(12)	114.6(4)
Ta(1)−N(2)	1.988(6)	Ta(1)−N(2)−Si(1)	128.9(3)
N(1)−C(1)	1.414(9)	Cl(1)−Ta(1)−N(1)	102.6(2)
N(2)−Si(1)	1.779(6)	Cl(1)−Ta(1)−N(2)	108.5(2)
N(2)−C(12)	1.450(9)	N(1)−Ta(1)−N(2)	98.8(2)
		Si(1)−N(2)−C(12)	116.4(4)

bending, giving rise to the relatively wide range of observed bond angles. In valence-bond terms, the nitrogen in linear imidos is sp-hybridized, resulting in a formally triple M−N bond. There are only a few reported examples of strongly bent imido complexes, and the bending in these is attributed either to the steric constraints of a chelate ring[40,48,49] or to electronic effects (in particular the absence of available empty metal d-orbitals of appropriate symmetry to interact with the nitrogen lone pair).[50,51] In the limiting case of a strongly bent imido ligand, the N atom would be sp^2-hybridized with a formally double M−N bond and a nonbonding electron pair localized on the nitrogen. There are also a number of linear imidos for which a formally triple M−N bond would result in a violation of the 18-electron rule, and such compounds are best described as possessing a double M−N bond.[44,46,52]

To the best of our knowledge, compound **4** is the most strongly bent transition metal imido complex reported so far. We attribute the observed bending to the steric restrictions imposed on the imido linkage by the chelating biphenyl ligand. The Ta=N bond is rather long compared to the typical range 1.6−1.8 Å for organoimido complexes of tantalum[31,32] but is comparable to the long Ta=N bond of 1.831(10) Å found in $Cp^*_2Ta(=NC_6H_5)H$,[44,52] which is considered to possess a Ta−N bond order between 2 and 3.

Reaction of **4** with MeMgBr in Et_2O gave the methyl derivative **5**, isolated in 85% yield as orange-red crystals from pentane (eq 2). The Ta*Me* group gives rise to a new singlet at 0.72 ppm in the ^{1}H NMR spectrum and a signal at 39.5 ppm in the ^{13}C NMR spectrum. Unfortunately, we have not been able to definitively identify Ta=N stretches in infrared spectra of **4** and **5**, presumably because they are coupled with other vibrations in the molecules.[32,53]

Reactivity of 4 and 5 toward Small Molecules. While many transition metal imido complexes are stable and unreactive, some exhibit high reactivities toward electrophiles,[54,55] nucleophiles,[56] or both.[32,45,57] Nucleophilic imido ligands tend to be associated with the early transition metals (and more strongly polarized M−N bonds), while later transition metals exhibit more covalent metal−nitrogen bonding and less nucleophilic imido nitrogen centers.[32,45] In addition, some imido complexes have been observed to react with unsaturated substrates, to give [2 + 2] or [2 + 4] cycloaddition products,[37,41,55] and certain d^0 imido complexes have been found to activate the C−H bonds in hydrocarbons.[35,37,39,58] It is expected, according to the bonding model described above, that bending of the imido ligand should lead to a reduced metal−nitrogen bond order and localization of a lone pair on nitrogen. This should lead to increased nucleophilicity of the imido nitrogen atom and increased reactivity of the complex due to a weaker, and more exposed, Ta=N bond.

Contrary to these expectations, our studies of compound **4** indicate that it is rather stable. This compound does not decompose in refluxing toluene-d_8 for 24 h and does not react with H_2, CO, C_2H_4, PhC≡CPh, or Me_3SiC≡CH within 24 h in refluxing benzene-d_6. The methyl derivative **5** also did not react with H_2 or Me_3SiC≡CH under similar conditions. Both **4** and **5** are inert toward the nucleophiles PPh_3, $PhPH_2$, and *p*-(*N*,*N*-dimethylamino)pyridine (24 h, 80 °C, benzene-d_6). Although transition-metal imido complexes typically react readily with organic carbonyl compounds,[32] no reaction was observed between **4** or **5** and benzophenone (4 h, 80 °C, benzene-d_6). Benzaldehyde reacted slowly with **4** (ca. 40% conversion after 20 h) and with **5** (70% conversion after 24 h) at room temperature in benzene-d_6 to give a mixture of products. Complexes **4** and **5** also reacted with weak acids such as PhOH and *p*-toluidine (but not with the more sterically hindered Ph_2-NH), giving mixtures of products.

Complex **5** reacts very slowly with carbon monoxide under 40−80 psi, at 80 °C in benzene. However, the accumulation of decomposition products prevented us from isolating and identifying the product of this reaction. While **4** did not react with xylyl isonitrile, compound **5** was found to undergo a clean reaction at room temperature to give the insertion product **6** (eq 3), isolated as bright yellow crystals in 68% yield.

The structure of **6** was determined by X-ray crystallography (Figure 2). Selected bond lengths and angles are listed in Table 2. The imido Ta−N(1)−C(1) bond angle of 133.2(3)° is considerably expanded relative to the corresponding value for **4**, while the bite angle of the chelating ligand (N(1)−Ta−N(2) = 94.2(2)°) is slightly reduced from that in **4**. These metrical changes may be attributed to the higher coordination number for the metal center, which leads to increased steric crowding

(48) Herrmann, W. A.; Marz, D. W.; Herdtweck, E. *Z. Naturforsch.* **1991**, *46b*, 747.
(49) Minelli, M.; Carson, M. R.; Whisenhunt, D. W., Jr.; Imhof, W.; Huttner, G. *Inorg. Chem.* **1990**, *29*, 4801.
(50) Haymore, B. L.; Maatta, E. A.; Wentworth, R. A. D. *J. Am. Chem. Soc.* **1979**, *101*, 2063.
(51) Gibson, V. C.; Marshall, E. L.; Redshaw, C.; Clegg, W.; Elsegood, M. R. J. *J. Chem. Soc., Dalton Trans.* **1996**, *21*, 4197.
(52) Parkin, G. P.; van Asselt, A.; Leahy, D. J.; Whinnery, L.; Hua, N. G.; Quan, R. W.; Henling, L. M.; Schaefer, W. P.; Santarsiero, B. D.; Bercaw, J. E. *Inorg. Chem.* **1992**, *31*, 82.
(53) Korolev, A. V.; Rheingold, A. L.; Williams, D. S. *Inorg. Chem.* **1997**, *36*, 2647.
(54) Maata, E. A.; Wentworth, R. A. D. *Inorg. Chem.* **1979**, *18*, 2409.
(55) Glueck, D. S.; Wu, J.; Hollander, F. J.; Bergman, R. G. *J. Am. Chem. Soc.* **1991**, *113*, 2041.
(56) Arndtsen, B. A.; Sleiman, H. F.; Chang, A. K.; McElwee-White, L. *J. Am. Chem. Soc.* **1991**, *113*, 4871.
(57) Arndtsen, B. A.; Sleiman, H. F.; McElwee-White, L. *Organometallics* **1993**, *12*, 2440.
(58) Cummins, C. C.; Baxter, S. M.; Wolczanski, P. T. *J. Am. Chem. Soc.* **1988**, *110*, 8731.

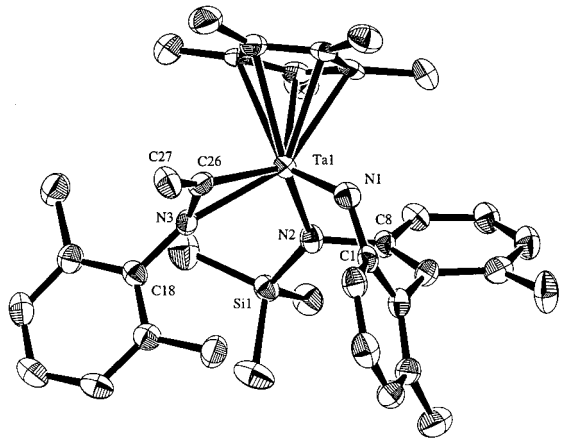

Figure 2. ORTEP diagram of Cp*Ta[=N($C_6H_3Me)_2$NSiMe_3][η^2-(2,6-$Me_2C_6H_3$)N=CMe] (**6**).

Table 2. Selected Bond Lengths (Å) and Angles (deg) for Compound **6**

Ta(1)−N(1)	1.819(4)	N(2)−Ta(1)−N(3)	89.2(1)
Ta(1)−N(2)	2.105(4)	N(2)−Ta(1)−C(26)	120.7(2)
Ta(1)−N(3)	2.259(4)	N(3)−Ta(1)−C(26)	33.5(2)
Ta(1)−C(26)	2.134(5)	Ta(1)−N(1)−C(1)	133.2(3)
Si(1)−N(2)	1.733(4)	Ta(1)−N(2)−Si(1)	133.8(2)
N(1)−C(1)	1.377(7)	Ta(1)−N(2)−C(8)	111.6(3)
N(2)−C(8)	1.452(6)	Si(1)−N(2)−C(8)	114.5(3)
N(3)−C(18)	1.437(6)	Ta(1)−N(3)−C(18)	163.6(3)
N(3)−C(26)	1.273(6)	Ta(1)−N(3)−C(26)	67.8(3)
C(26)−C(27)	1.487(7)	C(18)−N(3)−C(26)	124.2(4)
N(1)−Ta(1)−N(2)	94.2(2)	Ta(1)−C(26)−N(3)	78.6(3)
N(1)−Ta(1)−N(3)	110.6(2)	Ta(1)−C(26)−C(27)	152.1(4)
N(1)−Ta(1)−C(26)	95.1(2)	N(3)−C(26)−C(27)	127.2(4)

in **6** relative to **4**. The Ta−N(1) bond length, 1.819(4) Å, is slightly shorter than the Ta=N bond in **4**, which is consistent with the greater bond angle at N(1).

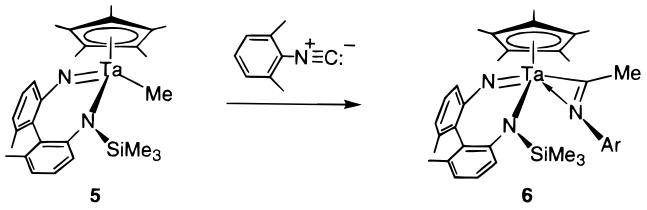

5 **6** (3)

The nucleophilic properties of the imido nitrogens in **4** and **5** were demonstrated by their reactions with MeI. Compound **4** did not react with MeI at room temperature in benzene-d_6, and upon heating, the reaction mixture gave a number of decomposition products. The methyl derivative **5**, on the other hand, reacts readily with MeI at room temperature. The product of this reaction (**7**), isolated as yellow crystals in 74% yield, is highly insoluble in nonpolar organic solvents (Et_2O, benzene) but is soluble in CH_2Cl_2. Reactions of imido complexes with MeI or MeBr have often been observed to result in complete cleavage of the metal−nitrogen bond to produce ammonium ions,[54,55] but spectroscopic characterization of **7** revealed that only 1 equiv of MeI had added to the Ta=N bond (eq 4). Furthermore, the insolubility of **7** in nonpolar solvents and the downfield shifts for the *Me*N−Ta group in the ^{1}H (3.39 ppm) and ^{13}C (53.4 ppm) NMR spectra suggested that **7** might be cationic, and this formulation was confirmed by X-ray crystallography.

An ORTEP drawing of **7** is shown in Figure 3, and selected bond distances and angles are given in Table 3. The Ta−I

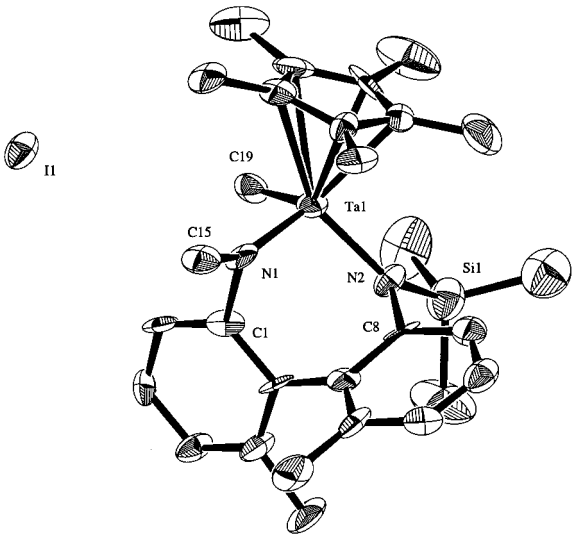

Figure 3. ORTEP diagram of {Cp*Ta[MeN($C_6H_3Me)_2$NSiMe_3]Me}$^+$I$^-$ (**7**).

Table 3. Selected Bond Lengths (Å) and Angles (deg) for Compound **7**

Ta(1)−I(1)	5.311(1)	N(1)−Ta(1)−N(2)	104.5(4)
Ta(1)−N(1)	1.92(1)	N(1)−Ta(1)−C(19)	102.0(5)
Ta(1)−N(2)	1.99(1)	N(2)−Ta(1)−C(19)	106.3(5)
Ta(1)−C(19)	2.14(2)	Ta(1)−N(1)−C(1)	101.8(8)
N(1)−C(1)	1.47(1)	Ta(1)−N(1)−C(15)	147.2(9)
N(1)−C(15)	1.45(2)	C(1)−N(1)−C(15)	111(1)
N(2)−C(8)	1.43(2)	Ta(1)−N(2)−C(8)	112.1(8)
N(2)−Si(1)	1.78(1)	Ta(1)−N(2)−Si(1)	133.4(6)
		Si(1)−N(2)−C(8)	114.5(9)

distance of 5.311(1) Å and the undistorted three-legged piano stool geometry about the metal center confirmed that the iodide is not coordinated to Ta. The unusually large Ta−N(1)−C(15) bond angle of 147.2(9)° and the small Ta−N(1)−C(1) angle of 101.8(8)° can be attributed to steric crowding caused by the MeN group interacting with the Cp* ring and probably the presence of a bonding interaction involving the *ipso* carbon, leading to a close Ta···C(1) contact of 2.64(1) Å.

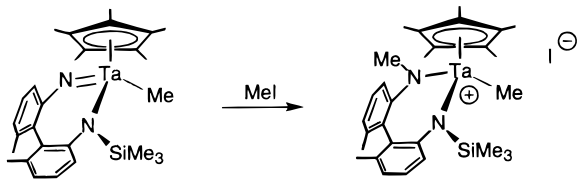

5 **7** (4)

We attribute the ionic structure of **7** to steric crowding about Ta, which prevents coordination of the iodide anion. The stability of the cation can also be rationalized by the possibility for stabilization by donation of π-electron density from the two amido nitrogens. While coordinatively unsaturated, cationic early transition metal complexes are potentially active as olefin polymerization catalysts, compound **7** did not react with ethene over 24 h (room temperature, dichloromethane-d_2).

Reactions of 4 and 5 with Silanes. Compounds **4** and **5** were found to react with hydrosilanes, to form tantalum hydride complexes via addition of the Si−H bond across the Ta=N bond. While the primary silanes $PhSiH_3$ and $PhCH_2SiH_3$ reacted at measurable rates at room temperature, reactions with most secondary silanes (such as $PhMeSiH_2$) could be observed only after prolonged heating, which led to decomposition and the formation of $HSiMe_3$ (by ^{1}H NMR spectroscopy). The tertiary

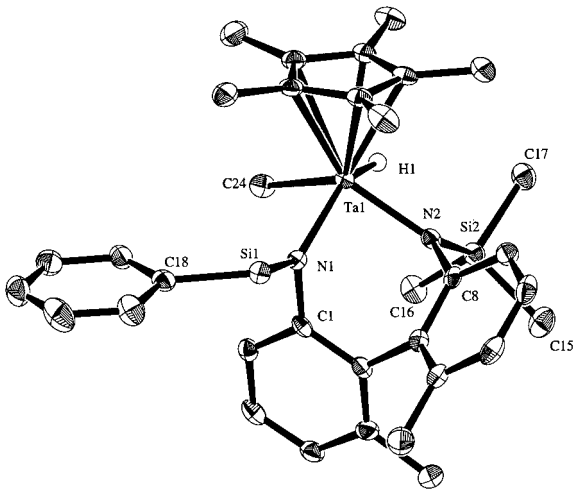

Figure 4. ORTEP diagram of Cp*Ta[$PhSiH_2N(C_6H_3Me)_2NSiMe_3$](H)-Me (**9**).

silane $MeEt_2SiH$ and the sterically hindered primary silane $MesSiH_3$ did not react with **4** even at 80 °C over 24 h in benzene-d_6. Addition of $PhSiH_3$ to **4** and **5** yielded the hydrido chloride and hydrido methyl complexes **8** and **9**, respectively, as shown in eq 5. The moderate rates of these reactions and the thermal instabilities of the products required use of neat $PhSiH_3$ and mild reaction conditions (room temperature) for isolation of the products.

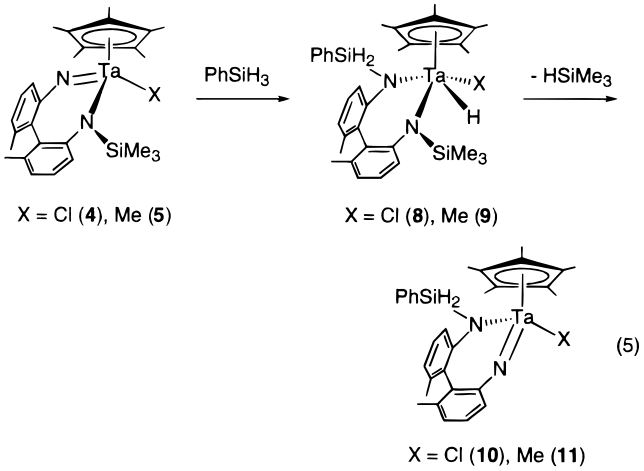

The TaH groups in **8** and **9** appear as singlets in the ^{1}H NMR spectra, at 20.44 and 17.15 ppm, respectively. The methyl ligand in **9** gives rise to a doublet in the ^{1}H NMR spectrum at 0.88 ppm, with coupling to the hydride ligand ($^3J_{HH} = 1.9$ Hz; coupling was not resolved for the TaH resonance). No significant changes were observed in the ^{1}H NMR spectrum of **9** on cooling to −80 °C. The Ta−H stretches in the IR spectra of **8** and **9** are observed at 1790 and 1778 cm^{-1}, respectively, and the deuteride **9**-d_3, prepared from **5** and $PhSiD_3$, exhibits a Ta-D stretch at 1278 cm^{-1}. No exchange of the hydride ligand in **9** was observed upon exposure to D_2 (1 atm, 25 °C, 24 h in benzene-d_6). Compound **9** also did not react with ethene under similar conditions.

The structure of **9** was determined by single-crystal X-ray crystallography (Figure 4 and Table 4). The tantalum adopts a four-legged piano stool coordination geometry, with approximately equal Ta−N(amide) distances of 2.060(3) and 2.028(3) Å. The hydride ligand H(1) was located in the Fourier difference map, and its position was refined. Interestingly, it adopts a position that is *trans* to the phenylsilyl group from which it is derived. The Ta−H(1) bond length in **9** is 1.67(3) Å. Similarly to compound **7**, the angles about N(1) show some deviation from the expected 120° for sp^2-hybridized N, with a Ta−N(1)−Si(1) angle of 136.0(1)° and a Ta−N(1)−C(1) angle of 113.8(2)°. This distortion is attributed to steric crowding associated with the Cp* ring. In contrast, the angles about N(2) do not deviate significantly from 120°.

Table 4. Selected Bond Lengths (Å) and Angles (deg) for Compound **9**

Ta(1)−N(1)	2.060(3)	N(2)−Si(2)−C(17)	113.5(1)
Ta(1)−N(2)	2.028(3)	C(15)−Si(2)−C(16)	105.8(2)
Ta(1)−H(1)	1.67(3)	C(15)−Si(2)−C(17)	105.2(2)
Ta(1)−C(24)	2.213(3)	C(16)−Si(2)−C(17)	111.8(2)
Si(1)−N(1)	1.731(3)	Ta(1)−N(1)−Si(1)	136.0(1)
Si(1)−C(18)	1.877(3)	Ta(1)−N(1)−C(1)	113.8(2)
Si(2)−N(2)	1.761(3)	Si(1)−N(1)−C(1)	109.7(2)
N(1)−C(1)	1.456(4)	Ta(1)−N(2)−Si(2)	122.9(1)
N(2)−C(8)	1.442(4)	Ta(1)−N(2)−C(8)	118.2(2)
N(1)−Ta(1)−N(2)	88.6(1)	Si(2)−N(2)−C(8)	118.3(2)
N(1)−Ta(1)−C(24)	87.8(1)	N(1)−Ta(1)−H(1)	138(1)
N(1)−Si(1)−C(18)	115.0(1)	N(2)−Ta(1)−H(1)	74(1)
N(2)−Si(2)−C(15)	108.0(1)	C(24)−Ta(1)−H(1)	70(1)
N(2)−Si(2)−C(16)	111.9(1)		

The Ta hydrides **8** and **9** are stable in the solid state under nitrogen and in the dark but slowly decompose in solution with clean elimination of $HSiMe_3$ (by ^{1}H NMR spectroscopy), to give the imido species **10** and **11**, respectively (eq 5). Other potential elimination products ($PhSiH_3$, $PhSiH_2Cl$, $PhMeSiH_2$, Me_3SiCl, or Me_4Si) were not observed in these decompositions. The hydrido chloride **8** begins to decompose after several hours in benzene-d_6 at room temperature, while the methyl hydride **9** is more stable and exhibits a half-life of a few days in benzene-d_6. Identification of **10** and **11** was based on their ^{1}H NMR spectra. Isolation of **11** was not possible as the elimination of $HSiMe_3$ from **9** did not go to completion but reached equilibrium, and attempts to remove the $HSiMe_3$ by prolonged reflux in benzene only resulted in production of a mixture of decomposition products.

In dichloromethane solution, the reaction of **4** with $PhSiH_3$ occurred over 4 days at room temperature, as the color of the reaction mixture slowly changed from dark red to orange to light yellow. The isolated pale yellow product (**12**) was found to possess a hydride ligand, observed by ^{1}H NMR spectroscopy as a doublet ($J = 6.0$ Hz) at 14.85 ppm in dichloromethane-d_2. Structural characterization of **12** by X-ray crystallography revealed the presence of a diamide ligand containing both $-SiH_2Ph$ and $-SiHClPh$ groups bound to the nitrogens (Figure 5). Relevant bond lengths and angles are listed in Table 5. The structure of **12** is similar to that of the methyl hydride **9**. Again, due to the steric hindrance of the Cp* ring, the angles at N(1) show significant deviation from 120°: the Ta−N(1)−Si(1) angle is 140.1(2)° and the Ta−N(1)−C(1) angle is 111.7(2)°. The hydride ligand, located in the Fourier difference map and refined isotropically, is 1.83(4) Å from tantalum (compared to the Ta−H bond length of 1.67(3) Å in **9**). In addition, the distance between H(1) and the neighboring silicon Si(2) in **12**, 1.86(4) Å, is rather small and significantly shorter than the sum of the van der Waals radii (ca. 3.1 Å), suggesting the presence of a nonclassical bonding interaction between these atoms. For comparison, the distance between the hydride H(1) and the silicon Si(2) of the Me_3Si group in **9** is 2.56(3) Å. The Ta−N(2)−Si(2) angle is reduced to 108.8(2)°, while in complexes **4**, **6**, **7**, and **9**, the corresponding Ta−N−Si angles are greater than 120°. Further support for a significant H(1)···Si(2) interaction is found in the bond distances and angles about Si(2), which suggest a distortion from tetrahedral geometry. The N(2)−Si(2)−C(21) angle of

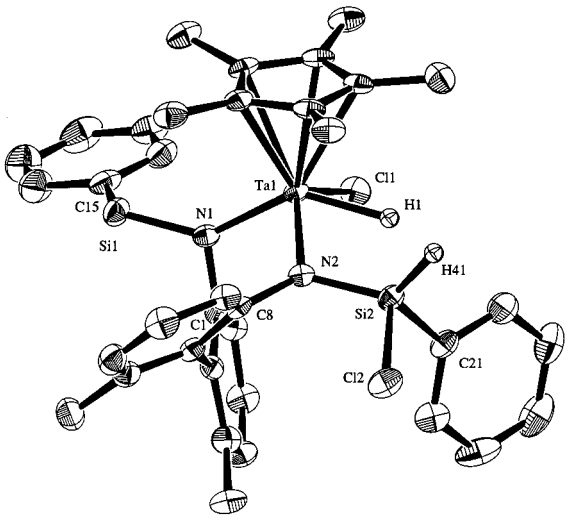

Figure 5. ORTEP diagram of Cp*Ta[PhSiH$_2$N(C$_6$H$_3$Me)$_2$NSiPhHCl]-(H)Cl (**12**).

Table 5. Selected Bond Lengths (Å) and Angles (deg) for Compound **12**

Ta(1)−Cl(1)	2.378(1)	N(1)−Ta(1)−H(1)	139(1)
Ta(1)−N(1)	2.015(3)	N(2)−Ta(1)−H(1)	67(1)
Ta(1)−N(2)	2.016(3)	N(1)−Si(1)−C(15)	113.0(2)
Ta(1)−H(1)	1.83(4)	Cl(2)−Si(2)−N(2)	103.1(1)
Cl(2)−Si(2)	2.149(2)	Cl(2)−Si(2)−C(21)	100.5(1)
Si(1)−N(1)	1.756(4)	N(2)−Si(2)−C(21)	120.2(2)
Si(1)−C(15)	1.877(4)	Cl(2)−Si(2)−H(41)	95(2)
Si(2)−N(2)	1.723(3)	C(21)−Si(2)−H(41)	112(2)
Si(2)−C(21)	1.873(4)	N(2)−Si(2)−H(41)	119(2)
Si(2)−H(41)	1.36(5)	Cl(2)−Si(2)−H(1)	174(1)
Si(2)−H(1)	1.86(4)	Ta(1)−N(1)−Si(1)	140.1(2)
N(1)−C(1)	1.450(5)	Ta(1)−N(1)−C(1)	111.7(2)
N(2)−C(8)	1.433(5)	Si(1)−N(1)−C(1)	108.1(3)
Cl(1)−Ta(1)−N(1)	92.29(9)	Ta(1)−N(2)−Si(2)	108.8(2)
Cl(1)−Ta(1)−N(2)	123.89(9)	Ta(1)−N(2)−C(8)	123.7(2)
N(1)−Ta(1)−N(2)	89.4(1)	Si(2)−N(2)−C(8)	127.4(3)
Cl(1)−Ta(1)−H(1)	76(1)		

120.2(2)° is consistent with the nitrogen and the phenyl group occupying equatorial positions in a distorted trigonal bipyramid. The chlorine atom appears to occupy an axial site, with Cl(2)−Si(2)−N(2) and Cl(2)−Si(2)−C(21) angles of 103.1(1)° and 100.5(1)°. The Si(2)−Cl(2) bond length of 2.149(2) Å is also rather long, approaching values observed for axial chlorine in pentacoordinate silicon compounds.[59] Similar nonclassical bonding interactions have been characterized for a number of transition metal hydrido silyl complexes,[60−67] based on short Si−H distances and distorted geometries at silicon. Such complexes can be viewed as exhibiting three-center M−H−Si bonding with limiting metal silyl hydride and η^2-H−Si resonance structures.[68] The bonding situation in compound **12** is different, since the silyl group is not directly bonded to the metal. Thus, the bonding in **12** is probably best described by the resonance structures shown in Scheme 1, involving a pentacoordinate Si center in one of the canonical forms. This interaction may also be differentiated from those found in a number of β-Si−H agostic complexes[69−71] in which an Si−H σ-bond is coordinated to the metal, without an increase of the coordination number at the silicon.

Scheme 1

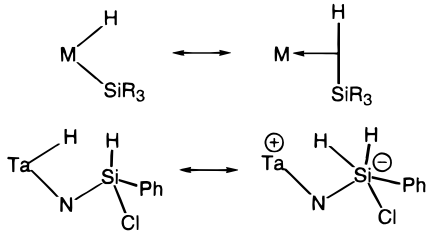

The existence of a bonding interaction between the hydride ligand and the neighboring silicon atom in **12** may also account for the low Ta−H stretching frequency (1678 vs 1790−1778 cm^{-1} for **8**, **9**, and **16**). Finally, evidence for such an interaction is seen in the unusually large ^{1}H NMR coupling constant (6.0 Hz) between H(1) and H(41) (the hydrogen bonded to Si(2)), which are otherwise separated by four bonds. The magnitude of this coupling and the appearance of the spectrum do not observably change on cooling to −80 °C (in dichloromethane-d_2). In the ^{29}Si (^{1}H coupled) NMR of **12**, the Ph*Si*H(Cl)N silicon appears as a doublet at −66.8 ppm ($^1J_{SiH}$ = 272 Hz) and the Ph*Si*H$_2$N silicon gives rise to a triplet at −26.9 ppm ($^1J_{SiH}$ = 208 Hz). Unresolved coupling ($J \approx 6-7$ Hz) to hydrogens of the phenyl groups was observed for both resonances, and this effect on the line width appears to obscure coupling to the hydride ligand.

The formation of **12** apparently involves a series of addition and elimination steps, combined with partial chlorination of a silicon atom. A possible mechanism is given in Scheme 2.

Monitoring the reaction by ^{1}H NMR spectroscopy provided evidence for some of the intermediates in this scheme. When **4** was reacted with excess PhSiH$_3$ (50 equiv) in dichloromethane-d_2, compound **8** was observed to form as an intermediate (the main TaH-containing species after 12 h) and then gradually disappear (complete conversion to **12** after 2 days). This reaction also produced Me$_3$SiCl and HSiMe$_3$ in a 1.2:1 ratio (by ^{1}H NMR integration). Another tantalum hydride signal, observed to grow and then decay during the reaction, is tentatively assigned to intermediate **13** (vide infra). Reaction of isolated **8** with PhSiH$_3$ in dichloromethane-d_2 (24 h, room temperature) also produced **12**, along with HSiMe$_3$, Me$_3$SiCl, and CHD$_2$Cl, identified by ^{1}H NMR spectroscopy. The formation of CHD$_2$Cl indicates that solvent is the source of the silicon-bound chlorine in **12**. Compound **10** was observed independently as resulting from the elimination of HSiMe$_3$ from **8** (benzene-d_6, room temperature), but the formation of both HSiMe$_3$ and Me$_3$SiCl suggests the intermediacy of **14** in an alternative pathway when the reaction occurs in dichloromethane (see Scheme 2). While a number of PhSi*H*$_2$ signals are observed

(59) Corriu, R. J. P.; Young, J. C. In *The Chemistry of Organic Silicon Compounds*; Patai, S., Rappoport, Z., Eds.; Wiley: New York, 1989; Vol. 2, p 1241.
(60) Nikonov, G. I.; Kuzmina, L. G.; Lemenovskii, D. A.; Kotov, V. V. *J. Am. Chem. Soc.* **1995**, *117*, 10133.
(61) Nikonov, G. I.; Kuzmina, L. G.; Lemenovskii, D. A.; Kotov, V. V. *J. Am. Chem. Soc.* **1996**, *118*, 6333.
(62) Spaltenstein, E.; Palma, P.; Kreutzer, K. A.; Willoughby, C. A.; Davis, W. M.; Buchwald, S. L. *J. Am. Chem. Soc.* **1994**, *116*, 10308.
(63) Jiang, Q.; Carroll, P. J.; Berry, D. H. *Organometallics* **1991**, *10*, 3648.
(64) Schubert, U.; Müller, J.; Alt, H. G. *Organometallics* **1987**, *6*, 469.
(65) Schubert, U.; Ackermann, K.; Wörle, B. *J. Am. Chem. Soc.* **1982**, *104*, 7378.
(66) Colomer, E.; Corriu, R. J. P.; Marzin, C.; Vioux, A. *Inorg. Chem.* **1982**, *21*, 368.
(67) Schubert, U. *Adv. Organomet. Chem.* **1990**, *30*, 151.
(68) Lichtenberger, D. L.; Rai-Chaudhuri, A. *J. Am. Chem. Soc.* **1990**, *112*, 2492.
(69) Procopio, L. J.; Carroll, P. J.; Berry, D. H. *J. Am. Chem. Soc.* **1994**, *116*, 177.
(70) Herrmann, W. A.; Huber, N. W.; Behm, J. *Chem. Ber.* **1992**, *125*, 1405.
(71) Herrmann, W. A.; Eppinger, J.; Spiegler, M.; Runte, O.; Anwander, R. *Organometallics* **1997**, *16*, 1813.

Scheme 2

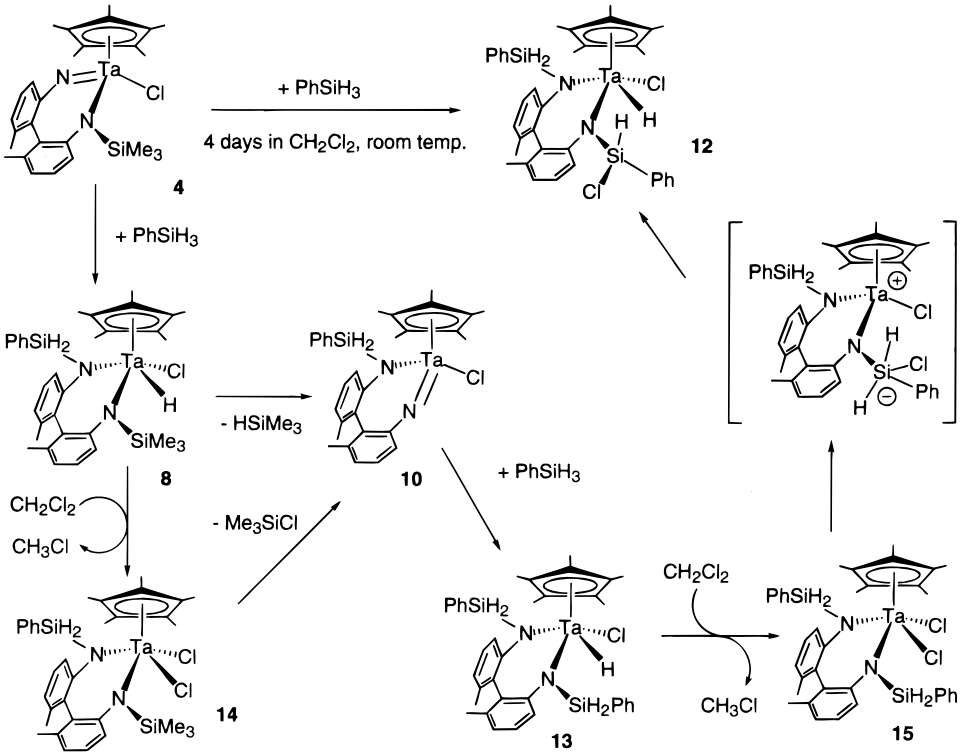

during the transformation (some associated with **10** and **13**), it is not possible to unambiguously assign resonances to species such as **14** and **15**.

In an attempt to isolate some of the intermediates in Scheme 2, and also to gain information concerning the silicon-chlorination step, the reaction of **8** with $PhSiH_3$ in benzene (3 days at room temperature) was examined. Removal of the volatiles from the resulting dark yellow solution and recrystallization of the residue from pentane afforded a yellow solid. The ^{1}H NMR spectrum (500 MHz, benzene-d_6) of this product mixture revealed a set of signals which represent a major component of the mixture and appear to be associated with **13**, the expected final product in the absence of CH_2Cl_2. The Ta*H* in **13** appears as a singlet at 19.76 ppm. One of the PhSiH_2 groups gives rise to two doublets ($^2J_{HH}$ = 10.1 Hz), while a set of signals assigned to the other PhSiH_2 group (two doublets of doublets) exhibits further small splittings of 3.1 and 1.5 Hz, presumably due to coupling to the Ta*H* hydride ligand. Other resonances for **13** were obscured by signals from other species. The elimination product **10** was also identified in this spectrum. Addition of dichloromethane-d_2 to this intermediate mixture resulted in its complete conversion to **12** after 16 h at room temperature, implying that **13** lies on the reaction pathway. Finally, a facile ligand exchange between Ta and Si via a pentacoordinate Si intermediate can be invoked to explain the migration of chlorine from tantalum to silicon. Evidence for the involvement of such intermediates in this system also comes from kinetic studies on the silane addition/elimination process (vide infra).

Kinetic Studies of the Silane Addition/Elimination Reactions. The kinetics of the $PhSiH_3$ addition to the tantalum imido complex **5** were studied by ^{1}H NMR spectroscopy at 35.0 °C (benzene-d_6 solvent). The disappearance of **5** in the presence of a large excess of the silane (25−70 equiv) was found to be first order in **5**, as shown by the linear decay of $\ln([\mathbf{5}]/[\mathbf{5}]_0)$ vs time. A plot of the observed pseudo-first-order rate constants k_{obs} vs $PhSiH_3$ concentrations (Figure 6) established a second-order rate law for the reaction and a rate constant of k_H = 5.57(6) × 10^{-5} L/(mol·s). The measured rate constant (k_{obs}) was not affected by addition of 1 equiv of the product (**9**).

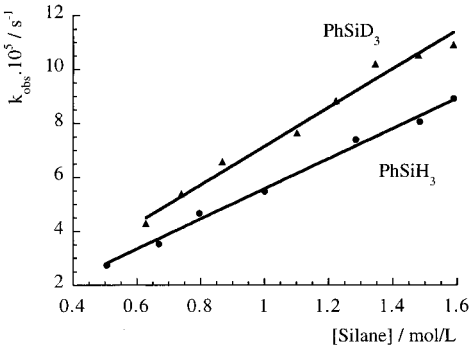

Figure 6. Observed pseudo-first-order rate constant for disappearance of **5** (k_{obs}) as a function of the phenylsilane concentration.

To gain more insight into the mechanism of the reaction of **5** with $PhSiH_3$, the H/D kinetic isotope effect was measured. The second-order rate constant for the reaction of **5** with $PhSiD_3$, measured under the same conditions, is k_D = 7.15(10) × 10^{-5} L/(mol·s), which corresponds to a kinetic isotope effect (KIE) of k_H/k_D = 0.78(1). This inverse isotope effect suggests that the rate-determining transition state does not involve significant breaking or making of bonds to hydrogen. Although it has been shown[72] that primary isotope effects can be very small or even inverse in cases of extremely exo- or endothermic reactions, this does not seem likely for the reaction under consideration. Inverse KIEs are usually secondary in nature and associated with changes in the bond strengths and the vibrational frequencies of bonds to H/D in the transition state.[73,74] We propose that the formation of an intermediate adduct, involving a pentacoordinate Si center, is the rate-determining step in the

(72) Melander, L. *Acta Chem. Scand.* **1971**, *25*, 3821.
(73) Streitwieser, A., Jr.; Jagow, R. H.; Fahey, R. C.; Suzuki, S. *J. Am. Chem. Soc.* **1958**, *80*, 2326.
(74) Melander, L.; Saunders, W. H. *Reaction Rates of Isotopic Molecules*; Wiley: New York, 1980.

Scheme 3

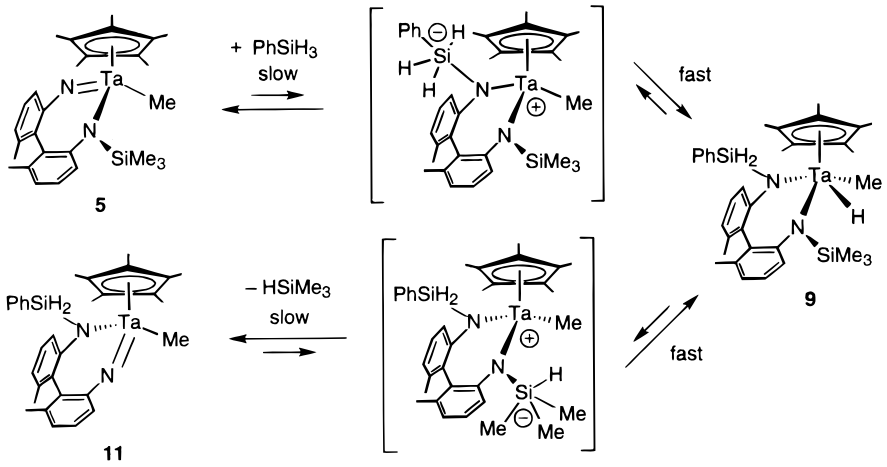

addition of the silane to the Ta imido complex **5**, as indicated in Scheme 3. Analogous pentacoordinate silicon species have often been invoked as intermediates in nucleophilic substitution at silicon,[59,75,76] and the formation of such intermediates has been shown in some cases to be the rate-determining step.[77] While no bonds to H/D are formed or broken in this step, an increase in the Si−H out-of-plane bending frequencies in the pentacoordinate Si intermediate relative to the free silane can lead to a larger zero-point energy difference between the proteated and the deuterated species in the transition state, relative to the zero-point energy difference in the reactants. Such an increase in the Si−H bending force constants can be explained by the increased "tightness" of the transition state relative to the reactants. The resulting lower activation barrier for the deuterated species is consistent with the observed inverse KIE. Related arguments have been used to explain the secondary isotope effects in the very extensively studied S_N2-type reactions at electrophilic sp^3 C centers, which proceed through a five-coordinate transition state.[73,74,78,79] We are not aware, however, of a similar observation of inverse secondary isotope effects for nucleophilic substitution reactions of hydrosilanes, although very small (1−1.3) primary kinetic isotope effects have been reported for nucleophilic substitution of the hydrogen in tertiary silanes with organolithium reagents.[77] Formation of the pentacoordinate Si intermediate is probably followed by a fast intramolecular hydride shift from Si to Ta to give product **9**. The observation of an H···Si bonding interaction in the related complex **12** further supports the idea that such a hydride shift can occur without a significant energy barrier, and thus cleavage of the Si−H bond is not a rate-determining step. Species analogous to **12** probably lie on the reaction coordinate of this migration.

An alternative, one-step mechanism can also be envisaged, involving a concerted [2 + 2] addition of the Si−H bond to the Ta═N bond, with a transition state resembling the structure of **12**. Such a mechanism, however, would be difficult to reconcile with the observed inverse isotope effect, since it would involve weakening of the bonds to H in the rate-determining transition state.

Additional evidence for rate-determining formation of a pentacoordinate silicon intermediate comes from the observation that silacyclobutane, $(CH_2)_3SiH_2$, reacts with **5** much faster than $PhSiH_3$, in contrast to other secondary silanes which were unreactive even at elevated temperatures. The disappearance of **5** in the presence of excess silane was followed by ^{1}H NMR spectroscopy, and the reaction was again found to follow a second-order rate law with a rate constant $k' = 1.23(2) \times 10^{-2}$ L/(mol·s) at 35.0 °C, which is 220 times greater than that for $PhSiH_3$. The product of this reaction, Cp*Ta[$(CH_2)_3$SiHN(C_6H_3-Me)$_2$NSiMe$_3$](H)Me (**16**), was isolated and characterized. Its ^{1}H and ^{13}C NMR spectra suggest a structure analogous to that for **8**, with the strained silacyclobutane ring remaining intact. The higher reactivity of this silane is therefore not due to release of ring strain in the reaction, but rather to the more favored formation of the intermediate with pentacoordinate silicon, which can readily accommodate an imposed 90° bond angle between axial and equatorial substituents in a trigonal bipyramid.

The lower kinetic barrier for addition of $(CH_2)_3SiH_2$ (compared to $PhSiH_3$) also results in relatively facile elimination of silacyclobutane from **16**. For comparison, compound **9** thermally decomposes exclusively via $HSiMe_3$ elimination and no $PhSiH_3$ was detected. For **16**, two competitive decomposition pathways were observed. Heating **16** for 4 h at 80 °C in benzene-d_6 resulted in about 50% decomposition of **16** to **17** and **5** in a ratio of 1.1:1 (eq 6; identification of **17** is based on its ^{1}H NMR spectrum). $HSiMe_3$ was also observed, but no free silacyclobutane could be detected in the reaction mixture, presumably due to its high reactivity leading to further reactions.

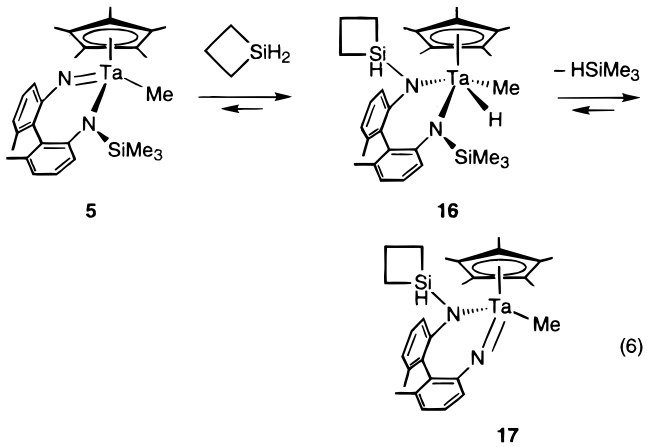

(6)

The kinetics of the $HSiMe_3$ elimination from **9**, presumed to occur via the mechanistic reverse of silane addition to **5**, were

(75) Sommer, L. H. *Stereochemistry, Mechanism and Silicon*; McGraw-Hill: New York, 1965.
(76) Corriu, R. J. P. *J. Organomet. Chem.* **1990**, *400*, 81.
(77) Corriu, R. J. P.; Henner, B. J. L. *J. Organomet. Chem.* **1975**, *102*, 407.
(78) Glad, S. S.; Jensen, F. *J. Am. Chem. Soc.* **1997**, *119*, 227.
(79) Poirier, R. A.; Wang, Y.; Westaway, K. C. *J. Am. Chem. Soc.* **1994**, *116*, 2526.

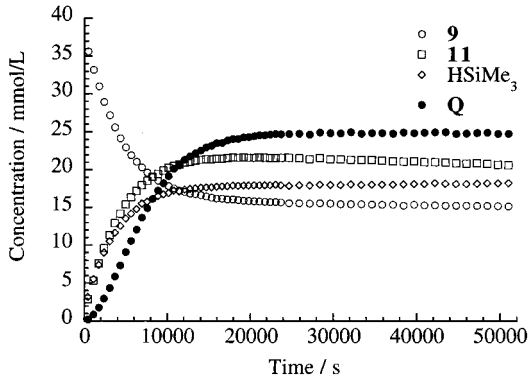

Figure 7. Plot of concentrations of **9**, **11**, and $HSiMe_3$ vs time for the elimination of $HSiMe_3$ from **9** (**Q** = [**11**][$HSiMe_3$]/[**9**]).

also studied by ^{1}H NMR spectroscopy. Figure 7, which is a plot of reactant and product concentrations and the ratio [**11**]-[$HSiMe_3$]/[**9**] as a function of time, shows that an equilibrium is established after about 7 h. From data taken during the time frame 8−14 h, the equilibrium constant was estimated to be $K_H = 0.025(2)$ mol/L. Note that a more accurate determination of K_H is not possible due to the slow decomposition of **11**, which is reflected in an estimated systematic error in K_H of ca. 10%. For an initial period (2000−3000 s at 60.6 °C), the plot of ln-[**9**]/[**9**]$_0$ vs time gave a straight line with a slope independent of the initial concentration of **9** over a broad concentration range (0.0052−0.041 mol/L). This implies a first-order rate law for the forward reaction. The rate constant, calculated from the average of five measurements, was found to be $k_H = 1.09(2) \times 10^{-4}$ s^{-1}.

The first-order rate constant for elimination of $DSiMe_3$ from **9**-d_3 at 60.6 °C was measured to be $k_D = 1.28(2) \times 10^{-4}$ s^{-1} (average of five runs); therefore, the deuterium KIE for this reaction is $k_H/k_D = 0.85(2)$. This inverse isotope effect again suggests that no bonds to H/D are being broken in the rate-determining step, which is consistent with our hypothesis of an intermediate pentacoordinate Si species. Such an intermediate is likely formed in a preequilibrium with the starting material (**9**), by a rapid hydride shift from Ta to Si. A rate-determining cleavage of the N−Si bond to liberate $HSiMe_3$ would then lead to product (see Scheme 3). Deuterium substitution appears to shift the preequilibrium toward the intermediate, as a result of the stronger Si−H (vs Ta−H) bond. Thus, the difference in relative zero-point energies for the Si−D and Si−H (vs the Ta-D and Ta−H) bonds results in an equilibrium isotope effect. The secondary isotope effect for the $HSiMe_3$-dissociation step, which is expected to be normal and small, apparently does little to offset the preequilibrium isotope effect. The net result is again a lower activation energy for reaction of the deuterated species, in agreement with the observed inverse KIE. The equilibrium constant for the reaction was estimated to be $K_D = 0.026(3)$ mol/L. While it can be expected that deuterium substitution will shift the equilibrium toward **11** + $DSiMe_3$, the difference between K_H and K_D is clearly within experimental error, and we are therefore prevented from drawing further quantitative conclusions about the equilibrium isotope effect or the isotope effect for the reverse reaction.

The temperature dependence on the first-order rate constant for elimination of $HSiMe_3$ from **9** was investigated by conducting the reaction at five different temperatures between 25.0 and 75.0 °C. A plot of ln(k/T) vs 1/T produced a straight line from which the activation parameters $\Delta H^{\ddagger} = 25.5(3)$ kcal/mol and $\Delta S^{\ddagger} = -0.3(1.0)$ cal/(mol·K) were extracted. The very small entropy of activation can be rationalized as resulting from the combined influences of a small positive value for the dissociative, rate-determining step (with an early transition state), and a small negative entropy change for the preequilibrium (more restricted rotation about the N−Si bond in the intermediate compared to that in the starting material).

Conclusions

In our exploration of the chemistry of some Ta complexes with C_2-symmetric silylamido ligands, we have observed cleavage of the N−Si bond and loss of a silyl group, to form Ta═N multiply bonded species. These highly bent tantalum imidos are rather stable, but react with silanes via an interesting two-step process involving an intermediate which features a pentacoordinate silicon center. Thus, the bending of an imido ligand in this system appears to enhance the nucleophilicity of the nitrogen center. Formation of pentacoordinate intermediates has often been invoked for reactions of silanes with nucleophiles,[59,75−77] but this is the first documented example of the involvement of such species in the addition/elimination reactions of silanes with transition metal imidos. The mechanism of these transformations appears to reflect the tendency of silicon to easily expand its coordination sphere and is thus rather different from that of C−H bond activations by zirconium or tantalum imidos,[35,39] as might be expected in view of the fundamental differences between carbon and silicon. The tendency of silicon to expand its coordination sphere is also exhibited in the nonclassical bonding interaction found in compound **12**. The loss of silyl groups in such tantalum complexes seems to be facilitated by the sterically crowded coordination environment created by the chelating ligand, and this steric crowding is also reflected in the ease of formation of the cationic complex **7**.

Experimental Section

General. All reactions with air-sensitive compounds were performed under dry nitrogen, using standard Schlenk and glovebox techniques. Reagents were obtained from commercial suppliers and used without further purification, unless otherwise noted. Olefin-free pentane, benzene, and toluene were prepared by pretreating with concentrated H_2SO_4, 0.5 N $KMnO_4$ in 3 M H_2SO_4, $NaHCO_3$, and finally anhydrous $MgSO_4$. Solvents (pentane, diethyl ether, benzene, toluene, and tetrahydrofuran) were distilled under nitrogen from sodium benzophenone ketyl. Benzene-d_6 was distilled from Na/K alloy. Dichloromethane-d_2 was distilled under nitrogen from calcium hydride. Commercial silanes were distilled and dried over molecular sieves before use. $PhSiD_3$ was prepared by reduction of $PhSiCl_3$ with $LiAlD_4$ (Aldrich, 98% D). ^{n}BuLi was used as a 1.6 M solution in hexanes and MeMgBr as a 1.4 M solution in Et_2O, as supplied by Aldrich. 2,2′-Diamino-6,6′-dimethylbiphenyl (**1**)[42] and Cp*$TaCl_4$[80] were prepared according to published literature procedures. NMR spectra were recorded at 300 or 500 MHz (^{1}H) with Bruker AMX-300 and DRX-500 spectrometers, at 100 MHz (^{13}C{^{1}H}) with an AMX-400 spectrometer, or at 99.4 MHz (^{29}Si) with a DRX-500 spectrometer, at ambient temperature and in benzene-d_6, unless otherwise noted. Signal multiplicities are reported as follows: s, singlet; d, doublet; t, triplet; q, quartet; qn, quintet; m, multiplet. Elemental analyses were performed by the Microanalytical Laboratory at UC Berkeley. Infrared spectra were recorded with a Mattson Instruments Galaxy Series FTIR spectrometer, as Nujol mulls with CsI plates or as KBr pellets.

***N,N′*-Bis(trimethylsilyl)-2,2′-diamino-6,6′-dimethylbiphenyl (2).** To a cold (0 °C) solution of **1** (7.75 g; 36.5 mmol) in THF (100 mL) was added dropwise 48 mL (76.8 mmol) of 1.6 M ^{n}BuLi. A white precipitate formed initially but dissolved completely after all of the ^{n}BuLi had been added. The solution was stirred at 0 °C for 2 h and was then allowed to warm to room temperature, resulting in a color change from pale yellow to green. Me_3SiCl (10.2 mL, 80.4 mmol) was then added dropwise. A white precipitate formed immediately,

(80) Yasuda, H.; Okamoto, T.; Nakamura, A. In *Organometallic Syntheses*; Eisch, J. J., King, R. B., Eds.; Academic Press: New York, 1965; Vol. 4, p 22.

and the evolution of heat was observed. After 2 h of heating at reflux, the solution was stirred overnight at room temperature. The THF was removed under vacuum to give an oily white solid. Extraction with pentane (2 × 100 mL) gave a bright yellow solution which was concentrated in vacuo until crystals appeared and then cooled to −78 °C. The resulting crystalline product was recrystallized from pentane and dried to afford 10.93 g (30.6 mmol, 84% yield) of the product as colorless crystals, mp 66.5−67.5 °C. ^{1}H NMR: δ 7.15 (t, overlaps with solvent peak, J = 7.8 Hz), 6.87 (d, 2 H, J = 7.8 Hz), 6.77 (d, 2 H, J = 7.5 Hz biphenyl H's), 3.53 (br s, 2 H, N*H*), 2.02 (s, 6 H, *Me*), 0.06 (s, 18 H, Si*Me*$_3$). ^{13}C{^{1}H} NMR: δ 146.3, 138.7, 129.2, 125.2, 120.5, 113.5 (aromatic C's), 20.5 (*Me*), 0.2 (Si*Me*$_3$). IR (Nujol, cm^{-1}): 3371 (m), 1579 (m), 1301 (s), 1252 (s), 962 (m), 868 (s), 840 (s), 773 (m), 750 (m). Anal. Calcd for $C_{20}H_{32}N_2Si_2$: C, 67.35; H, 9.04; N, 7.85. Found: C, 67.15; H, 9.21; N, 7.78.

Li(Me$_3$Si)N(C$_6$H$_3$Me)$_2$N(SiMe$_3$)Li (3). To a solution of 10.87 g (30.48 mmol) of **2** in 150 mL of pentane at 0 °C was added dropwise 40.0 mL (64.0 mmol) of 1.6 M ^{n}BuLi. Formation of a white precipitate was observed within 1 h. The mixture was allowed to warm to room temperature and was stirred overnight, during which time the precipitate gradually dissolved. The slightly cloudy solution was filtered, concentrated in vacuo, and cooled to −78 °C to afford 5.02 g of the product as white crystals (mp 120−125 °C, dec). Concentration and cooling of the filtrate afforded another 2.02 g of product, for a total yield of 63%. ^{1}H NMR: δ 6.98 (t, 2 H, J = 7.7 Hz), 6.71 (d, 2 H, J = 7.8 Hz), 6.61 (d, 2 H, J = 7.3 Hz, biphenyl H's), 1.75 (s, 6 H, *Me*), 0.06 (s, 18 H, Si*Me*$_3$). ^{13}C{^{1}H} NMR: δ 159.4, 139.2, 133.6, 130.1, 127.1, 120.6 (aromatic C's), 21.0 (*Me*), 3.7 (Si*Me*$_3$). IR (Nujol, cm^{-1}): 3053 (m), 1571 (s), 1562 (s), 1269 (s), 1255 (s), 1245 (s), 1038 (s), 958 (s), 856 (s), 825 (s), 793 (s), 746 (s), 582 (m), 569 (m), 472 (m), 455 (m). Anal. Calcd for $C_{20}H_{30}N_2Si_2Li_2$: C, 65.18; H, 8.21; N, 7.60. Found: C, 63.84; H, 8.94; N, 5.76. Satisfactory elemental analysis data could not be obtained, even after repeated recrystallization of the spectroscopically pure compound.

Cp*Ta[=N(C$_6$H$_3$Me)$_2$NSiMe$_3$]Cl (4). Cp*TaCl$_4$ (3.43 g, 7.48 mmol) and **3** (2.76 g, 7.48 mmol) were dissolved in 150 mL of benzene, and the mixture was heated at reflux for 4 h, resulting in a dark red solution. After being cooled to room temperature, the solvent was removed under vacuum and the residual solid was extracted with about 200 mL of pentane until the extracts were colorless. The dark red pentane solution was concentrated to about 70 mL, which caused precipitation of red, prism-shaped crystals. After being cooled to −78 °C, the solution was filtered and the isolated crystals were washed with pentane and dried under vacuum to afford 3.21 g of **4** (68%, mp 176−179 °C). ^{1}H NMR: δ 7.26 (m, 1 H), 7.02 (m, 1 H), 6.91 (m, 1 H), 6.65 (m, 2 H), 6.58 (m, 1 H, aromatic H's), 2.04 (s, 3 H, *Me*), 2.04 (s, 3 H, *Me*), 1.89 (s, 15 H, *Me*$_5$C$_5$), 0.04 (s, 9 H, *Me*$_3$Si). ^{13}C{^{1}H} NMR (dichloromethane-d_2): δ 156.7, 140.1, 138.7, 135.9, 135.4, 128.1, 127.5, 127.3, 127.1, 123.5, 121.5, 121.2, 113.3 (aromatic C's), 21.0 (*Me*, *Me*′), 11.6 (*Me*$_5$C$_5$), 1.8 (*Me*$_3$Si). IR (KBr, cm^{-1}): 3049 (w), 2953 (m), 2916 (m), 1574 (m), 1446 (m), 1250 (s), 1211 (m), 1012 (m), 945 (m), 900 (m), 854 (s), 769 (m), 727 (m). Anal. Calcd for $C_{27}H_{36}N_2ClSiTa$: C, 51.23; H, 5.73; N, 4.43. Found: C, 51.21; H, 5.90; N, 4.34.

Cp*Ta[=N(C$_6$H$_3$Me)$_2$NSiMe$_3$]Me (5). To a solution of **4** (1.01 g, 1.59 mmol) in diethyl ether (80 mL) was added 1.20 mL of 1.4 M MeMgBr (1.68 mmol) at room temperature. The color of the solution gradually changed from dark red to light red-orange, with formation of a white precipitate. After being stirred for 5 h, the solvent was removed in vacuo and the residue was extracted with about 100 mL of pentane, until extracts were colorless. The pentane solution was concentrated to less than 10 mL and left at −78 °C for 12 h, to obtain 0.83 g of **5** as a bright red-orange crystalline powder (85% yield, mp 114−118 °C). ^{1}H NMR: δ 7.28 (m, 1 H), 7.05 (m, 1 H), 6.98 (m, 1 H), 6.69 (m, 2 H), 6.59 (m, 1 H, aromatic H's), 2.09 (s, 3 H, *Me*), 2.05 (s, 3 H, *Me*), 1.78 (s, 15 H, *Me*$_5$C$_5$), 0.72 (s, 3 H, *Me*Ta), −0.08 (s, 9 H, *Me*$_3$Si). ^{13}C{^{1}H} NMR: δ 159.2, 140.1, 139.5, 135.9, 133.5, 130.6, 128.8, 127.6, 127.4, 124.9, 120.9, 117.9, 113.6 (aromatic C's), 39.5 (*Me*Ta), 21.5 (*Me*), 21.3 (*Me*), 11.4 (*Me*$_5$C$_5$), 1.9 (*Me*$_3$Si). IR (KBr, cm^{-1}): 3045 (w), 2954 (m), 2912 (m), 1571 (m), 1446 (s), 1377 (w), 1281 (s), 1250 (s), 1207 (m), 1041 (w), 945 (w), 903 (m), 845 (s), 771 (m), 756 (m), 728 (m). Anal. Calcd for $C_{28}H_{39}N_2SiTa$: C, 54.89; H, 6.42; N, 4.57. Found: C, 54.24; H, 6.47; N, 4.21.

Cp*Ta[=N(C$_6$H$_3$Me)$_2$NSiMe$_3$][η^2-(2,6-Me$_2$C$_6$H$_3$)N=CMe] (6). A solution of xylyl isonitrile (0.12 g, 0.92 mmol) in 20 mL of pentane was added to a solution of **5** (0.57 g, 0.92 mmol) in 40 mL of pentane. The red, transparent solution was stirred for 12 h at room temperature, resulting in the formation of a bright yellow, crystalline precipitate which was filtered and dried in vacuo. Cooling the filtrate to −78 °C afforded a second crop of crystals, giving a total yield of 0.47 g of **6** (68% yield). The product was purified by recrystallization from Et$_2$O, which results in incorporation of 0.5 equiv of solvent in the crystals (mp > 180 °C, dec). ^{1}H NMR (400 MHz): δ 7.35 (m, 1 H), 7.21 (m, 1 H), 7.03 (m, 2 H), 6.85 (m, 2 H), 6.80 (m, 1 H), 6.52 (d, 1 H), 6.18 (d, 1 H, aromatic H's), 3.25 (q, 2 H, Et$_2$O), 2.18 (s, 3 H, *Me*), 2.16 (s, 3 H, *Me*), 2.05 (s, 3 H, *Me*), 1.94 (s, 15 H, *Me*$_5$C$_5$), 1.86 (t, 3 H, *Me*), 1.26 (s, 3 H, N=C-*Me*), 1.11 (t, 3 H, Et$_2$O), 0.03 (s, 9 H, *Me*$_3$Si). ^{13}C-{^{1}H} NMR: δ 255.0 (N=*C*-Me), 158.2, 154.7, 145.8, 138.5, 136.1, 135.8, 131.7, 129.9, 129.3, 129.0, 128.5, 127.1, 126.9, 126.6, 125.3, 125.2, 120.5, 116.8, 112.1 (aromatic C's), 66.2 (Et$_2$O), 23.1, 22.0, 21.3, 19.9, 19.2, 15.9, 12.3 (*Me*'s), 5.2 (*Me*$_3$Si). IR (KBr, cm^{-1}): 3043 (w), 2953 (m), 2916 (m), 1579 ($\nu_{N=C}$, m), 1446 (s), 1313 (s), 864 (s), 837 (s), 773 (m). Anal. Calcd for $C_{39}H_{53}N_3O_{0.5}SiTa$: C, 59.99; H, 6.84; N, 5.38. Found: C, 59.88; H, 7.01; N, 5.18.

{Cp*Ta[MeN(C$_6$H$_3$Me)$_2$NSiMe$_3$]Me}$^+$I$^-$ (7). To a solution of **5** (0.46 g, 0.75 mmol) in 20 mL of Et$_2$O was added 3 mL of MeI at room temperature. The mixture instantly became cloudy. After the mixture was stirred for 24 h, the yellow precipitate was filtered off, washed with 20 mL of Et$_2$O and then 20 mL of pentane, and finally dried under vacuum to afford 0.42 g (74% yield; mp 240−243 °C, dec, subl) of **7** as a yellow, microcrystalline powder. ^{1}H NMR (dichloromethane-d_2): δ 7.52 (m, 2 H), 7.39 (m, 1 H), 7.29 (m, 1 H), 7.21 (m, 1 H), 6.99 (m, 1 H, aromatic H's), 3.39 (s, 3 H, *Me*N), 2.19 (s, 15 H, *Me*$_5$C$_5$), 2.16 (s, 3 H, *Me*), 2.10 (s, 3 H, *Me*), 0.78 (s, 3 H, Ta*Me*), −0.08 (s, 9 H, *Me*$_3$Si). ^{13}C{^{1}H} NMR (dichloromethane-d_2): δ 141.1, 138.5, 138.4, 135.0, 134.2, 132.3, 131.7, 131.3, 131.0, 130.0, 128.8, 127.4, 124.0 (aromatic C's), 55.1 (*Me*Ta), 53.4 (*Me*N), 21.4 (*Me*), 20.4 (*Me*), 12.4 (*Me*$_5$C$_5$), 1.5 (*Me*$_3$Si). IR (KBr, cm^{-1}): 2953 (m), 2916 (m), 1581 (w), 1443 (m), 1381 (w), 1250 (m), 839 (s). Anal. Calcd for $C_{29}H_{42}N_2ISi_2Ta$: C, 46.16; H, 5.61; N, 3.71. Found: C, 45.81; H, 5.59 N, 3.75.

Cp*Ta[PhSiH$_2$N(C$_6$H$_3$Me)$_2$NSiMe$_3$](H)Cl (8). A solution of **4** (0.56 g, 0.88 mmol) in 1.5 mL of neat PhSiH$_3$ was stirred at room temperature. The inhomogeneous red mixture turned light yellow after 1 day. The volatile material was removed under vacuum, the resulting residue was washed with pentane (2 × 20 mL) and extracted with toluene (about 70 mL). The toluene solution was concentrated to 10 mL and cooled to −78 °C, and the resulting precipitate was washed with pentane, to obtain 0.39 g of **8** (in two crops, 60% yield) as a pale yellow powder (mp 138−141 °C, dec). The product is weakly light-sensitive and is best kept in the dark. ^{1}H NMR: δ 20.44 (s, 1 H, Ta*H*), 7.76 (m, 2 H), 7.60 (m, 1 H), 7.08 (m, 5 H), 6.95 (m, 1 H), 6.80 (m, 2 H, aromatic H's), 5.46 (d, 1 H, $^2J_{HH}$ = 9.8 Hz, $^1J_{HSi}$ = 195 Hz, PhSi*H*$_2$N), 4.80 (d, 1 H, $^2J_{HH}$ = 9.8 Hz, $^1J_{HSi}$ = 201 Hz, PhSi*H*$_2$N), 2.10 (s, 3 H, *Me*), 2.04 (s, 3 H, *Me*), 2.02 (s, 15 H, *Me*$_5$C$_5$), 0.03 (s, 9 H, *Me*$_3$Si). ^{13}C{^{1}H} NMR: δ 156.9, 151.5, 138.6, 136.8, 136.0, 135.7, 134.2, 130.4, 129.7, 128.9, 127.3, 127.1, 126.6, 126.3, 126.1, 123.7, 121.0 (aromatic C's), 21.4 (*Me*), 20.7 (*Me*), 13.3 (*Me*$_5$C$_5$), 4.7 (*Me*$_3$-Si). IR (KBr, cm^{-1}): 3055 (w), 2987 (m), 2916 (m), 2216 and 2150 (ν_{Si-H}, s), 1790 (ν_{Ta-H}, m), 1564 (m), 1433 (s), 1238 (s), 1213 (s), 1111 (m), 955 (m), 910 (m), 850 (s). Anal. Calcd for $C_{33}H_{44}N_2ClSi_2$-Ta: C, 53.47; H, 5.98; N, 3.78. Found: C, 53.84; H, 6.10; N, 3.73.

Cp*Ta[PhSiH$_2$N(C$_6$H$_3$Me)$_2$NSiMe$_3$](H)Me (9). A solution of **5** (0.37 g, 0.60 mmol) in 0.5 mL of neat PhSiH$_3$ was stirred at room temperature for 1 day. The clear, bright red-orange mixture gradually turned pale yellow, with the formation of a precipitate. The volatile material was removed under vacuum, and the residue was extracted with Et$_2$O (80 mL). The extract was filtered, concentrated to about 10 mL, and cooled to −78 °C. The resulting white crystalline precipitate was isolated, recrystallized again from Et$_2$O, washed with cold pentane, and dried under vacuum to obtain 0.25 g of **9** (58%; mp 148−149 °C,

dec). The product is weakly light-sensitive and is best kept in the dark. ^{1}H NMR: δ 17.15 (s, 1 H, Ta*H*), 7.49 (m, 2 H), 7.10 (m, 5 H), 6.98 (m, 1 H), 6.94 (m, 1 H), 6.83 (m, 2 H, aromatic H's), 5.29 (d, 1 H, $^2J_{HH}$ = 9.6 Hz, $^1J_{HSi}$ = 179 Hz, PhSi*H*$_2$N), 4.68 (d, 1 H, $^2J_{HH}$ = 9.6 Hz, $^1J_{HSi}$ = 184 Hz, PhSi*H*$_2$N), 2.11 (s, 3 H, *Me*), 2.08 (s, 3 H, *Me*), 1.91 (s, 15 H, *Me*$_5$C$_5$), 0.88 (d, 3 H, $^3J_{HH}$ = 1.9 Hz, *Me*Ta), 0.00 (s, 9 H, *Me*$_3$Si). ^{13}C{^{1}H} NMR: δ 156.3, 153.4, 138.3, 137.3, 136.6, 135.5, 134.7, 134.3, 130.2, 128.5, 127.1, 126.6, 126.6, 126.2, 125.2, 124.6, 116.2 (aromatic C's), 48.4 (*Me*Ta), 21.5 (*Me*), 21.0 (*Me*), 12.7 (*Me*$_5$C$_5$), 4.6 (*Me*$_3$Si). IR (KBr, cm^{-1}): 3057 (w), 2958 (m), 2922 (m), 2214 and 2150 (ν_{Si-H}, m), 1778 (ν_{Ta-H}, m), 1564 (m), 1431 (m), 1236 (s), 948 (m), 910 (m), 870 (m), 845 (s). Characteristic IR bands for **9**-*d*$_3$: 1605 and 1565 (ν_{SiD}, m), 1278 (ν_{TaD}, m). Anal. Calcd for $C_{34}H_{47}N_2Si_2Ta$: C, 56.65; H, 6.57; N, 3.89. Found: C, 57.17; H, 6.68; N, 3.85.

Cp*Ta[PhSiH$_2$N(C$_6$H$_3$Me)$_2$NSiPhHCl](H)Cl (12). To a solution of **4** (1.00 g, 1.58 mmol) in 25 mL of CH_2Cl_2 was added 1.6 mL of $PhSiH_3$, and the mixture was stirred at room temperature. The solution slowly changed color from dark red through orange to yellow over a period of 4 days. The volatile material was removed under vacuum, and the residual solid was washed with pentane (2 × 25 mL) and dried to afford 1.08 g of **12** as a pale yellow powder (84%; mp 156−159 °C, dec). The crude product was purified by recrystallization from toluene. ^{1}H NMR (dichloromethane-*d*$_2$): δ 14.85 (d, 1 H, $^4J_{HH}$ = 6.0 Hz, Ta*H*), 7.1−7.5 (m, 8 H), 7.03 (m, 5 H), 6.88 (m, 1 H), 6.60 (m, 2 H, aromatic H's), 6.28 (d, 1 H, $^4J_{HH}$ = 6.0 Hz, PhSi*H*(Cl)N), 5.37 (d, 1 H, $^2J_{HH}$ = 10.4 Hz, PhSi*H*$_2$N), 4.54 (d, 1 H, $^2J_{HH}$ = 10.4 Hz, PhSi*H*$_2$N), 2.32 (s, 15 H, *Me*$_5$C$_5$), 2.01 (s, 3 H, *Me*), 1.98 (s, 3 H, *Me*). ^{13}C{^{1}H} NMR (benzene-*d*$_6$): δ 153.8, 149.8, 140.2, 138.6, 137.9, 135.7, 134.9, 134.2, 133.8, 133.7, 130.7, 129.4, 128.3, 127.9, 127.4, 127.1, 126.2, 126.2, 125.0, 122.3 (aromatic C's), 21.1 (*Me*), 20.7 (*Me*), 12.7 (*Me*$_5$C$_5$). ^{29}Si NMR (direct detection, 99.4 MHz, benzene-*d*$_6$): δ −26.9 (t, $^1J_{SiH}$ = 208 Hz, Ph*Si*H$_2$N), −66.8 (d, $^1J_{SiH}$ = 272 Hz, Ph*Si*HClN). IR (KBr, cm^{-1}): 3053 (w), 2999 (w), 2916 (w), 2189 and 2152 (ν_{Si-H}, m), 1678 (ν_{Ta-H}, w br), 1585 (w), 1566 (w), 1429 (m), 1113 (m), 835 (s). Anal. Calcd for $C_{36}H_{41}N_2Cl_2Si_2Ta$: C, 53.40; H, 5.10; N, 3.46. Found: C, 53.44; H, 5.12; N, 3.46.

Cp*Ta[(CH$_2$)$_3$SiHN(C$_6$H$_3$Me)$_2$NSiMe$_3$](H)Me (16). To a solution of **5** (0.37 g, 0.60 mmol) in 25 mL of pentane was added 0.1 mL of $(CH_2)_3SiH_2$, and the mixture was stirred overnight at room temperature. The solution color changed from orange-red to light yellow. The volatile material was removed in vacuo, and the resulting residue was redissolved in pentane (30 mL), concentrated, and crystallized at −78 °C to afford 0.25 g of **16** as a crystalline, off-white powder (60% yield). ^{1}H NMR: δ 17.02 (s, 1 H, Ta*H*), 7.12−7.04 (m, 3 H), 6.93 (m, 2 H), 6.79 (m, 1 H, aromatic H's), 5.14 (m, 1 H, Si*H*), 2.13 (s, 3 H, *Me*), 2.06 (s, 3 H, *Me*), 1.91 (s, 15 H, *Me*$_5$C$_5$), 1.60−1.40, 1.27−1.22 and 0.86−0.84 (m, 6 H, (C*H*$_2$)$_3$SiH), 0.75 (d, 3 H, $^3J_{HH}$ = 2.1 Hz, *Me*Ta), 0.01 (s, 9 H, *Me*$_3$Si). ^{13}C{^{1}H} NMR: δ 156.4, 153.0, 137.7, 137.2, 134.7, 134.4, 127.1, 126.4, 126.2, 125.9, 124.5, 124.3, 116.2 (aromatic C's), 48.4 (*Me*Ta), 21.1 (*Me*), 20.9 (*Me*), 20.5, 18.7, 15.1 ((*C*H$_2$)$_3$SiH), 12.6 (*Me*$_5$C$_5$), 4.5 (*Me*$_3$Si). IR (KBr, cm^{-1}): 3051 (w), 2960 (m), 2914 (m), 2154 (ν_{Si-H}, w), 1780 (ν_{Ta-H}, m), 1566 (w), 1437 (m), 1236 (s), 1118 (m), 916 (s), 841 (s). Anal. Calcd for $C_{31}H_{47}N_2Si_2Ta$: C, 54.37; H, 6.92; N, 4.09. Found: C, 54.59; H, 7.23; N, 4.12.

X-ray Structure Determinations. X-ray diffraction measurements were made on a Siemens SMART diffractometer with a CCD area detector, using graphite monochromated Mo Kα radiation. Details of the crystal structure determinations are given in the Supporting Information.

Kinetic Measurements. Reactions were monitored by ^{1}H NMR spectroscopy, with a Bruker AMX300 spectrometer, using 5 mm Wilmad NMR tubes, equipped with J. Young Teflon screw caps. The samples were frozen in liquid N_2 immediately after preparation and defrosted just before being placed in the preshimmed probe, which was preheated at the required temperature. The probe temperature was calibrated using an ethylene glycol sample[81] and monitored with a thermocouple. Repeated calibration showed that the temperature was maintained within ±0.2 °C of the set value. Single scan spectra were acquired automatically at preset time intervals. The peaks were integrated relative to ferrocene as an internal standard. Rate constants were obtained by nonweighted linear least-squares fits of the integrated first-order rate law in logarithmic form, $\ln C = \ln C_0 - k_{obs}t$. When several peaks from the same species were monitored, separate plots of $\ln C$ (as calculated from each signal) vs t were produced, and the rate constants (typically within two standard deviations from each other) were averaged. The activation enthalpy and entropy for the trimethylsilane elimination reaction were determined by weighted, linear least-squares fit of $\ln(k/T)$ vs $1/T$ at five different temperatures. The standard deviations in k and T at each data point were calculated on the basis of the random error of the multiple measurements combined with 5% estimated systematic error. Further details of the kinetic studies for each reaction are given in the Supporting Information.

Acknowledgment. The authors acknowledge the National Science Foundation for their generous support of this work. We also thank Professor Andrew Streitweiser for helpful discussions on isotope effects and Dr. Fred Hollander for assistance with the X-ray structrure determinations.

Supporting Information Available: Experimental data for the intermediates characterized only by ^{1}H NMR spectrosopy (**10**, **11**, **13**, and **17**), experimental details for the kinetic measurements, tables and plots of kinetic data, and tables of crystal, data collection, and refinement parameters, bond distances and angles, and anisotropic displacement parameters for **4**, **6**·$^1/_2$Et$_2$O, **7**, **9**, and **12** (60 pages). See any current masthead page for ordering and Internet access instructions.

JA9721982

(81) Ammann, C.; Meier, P.; Merbach, A. E. *J. Magn. Reson.* **1982**, *46*, 319.